ACS APPLIED MATERIALS & INTERFACES

Research Article

www.acsami.org

Curing of a Bisphenol E Based Cyanate Ester Using Magnetic Nanoparticles as an Internal Heat Source through Induction Heating

Jeremiah W. Hubbard,[†] François Orange,[‡] Maxime J.-F. Guinel,[‡,§] Andrew J. Guenthner,[⊥] Joseph M. Mabry,[⊥] Christopher M. Sahagun,[∥] and Carlos Rinaldi*[,†,¶]

[†]Department of Chemical Engineering, University of Puerto Rico—Mayagüez, Call Box 9000, Mayagüez, 00681-9000 Puerto Rico

[‡]Department of Physics and Nanoscopy Facility, College of Natural Sciences, University of Puerto Rico, P.O. Box 70377, San Juan, 00936-8377 Puerto Rico

[§]Department of Chemistry, College of Natural Sciences, University of Puerto Rico, P.O. Box 70377, San Juan, 00936-8377 Puerto Rico

[⊥]Aerospace Systems Directorate, Air Force Research Laboratory, 10 E. Saturn Boulevard, Edwards Air Force Base, California 93524, United States

[∥]National Research Council/Air Force Research Laboratory, 10 E. Saturn Boulevard, Edwards Air Force Base, California 93524, United States

[¶]J. Crayton Pruitt Family Department of Biomedical Engineering and Department of Chemical Engineering, University of Florida, P.O. Box 116131, Gainesville, Florida 32611, United States

Supporting Information

ABSTRACT: We report on the control of cyclotrimerization forming a polycyanurate polymer using magnetic iron oxide nanoparticles in an alternating-current (ac) field as an internal heat source, starting from a commercially available monomer. Magnetic nanoparticles were dispersed in the monomer and catalytic system using sonication, and the mixture was subjected to an alternating magnetic field, causing the magnetic nanoparticles to dissipate the energy of the magnetic field in the form of heat. Internal heating of the particle/monomer/catalyst system was sufficient to start and sustain the polymerization reaction, producing a cyanate ester network with conversion that compared favorably to polymerization through heating in a conventional laboratory oven. The two heating methods gave similar differential scanning calorimetry temperature profiles, conversion rates, and glass transition temperatures when using the same temperature profile. The ability of magnetic nanoparticles in an ac field to drive the curing reaction should allow for other reactions forming high-temperature thermosetting polymers and for innovative ways to process such polymers.

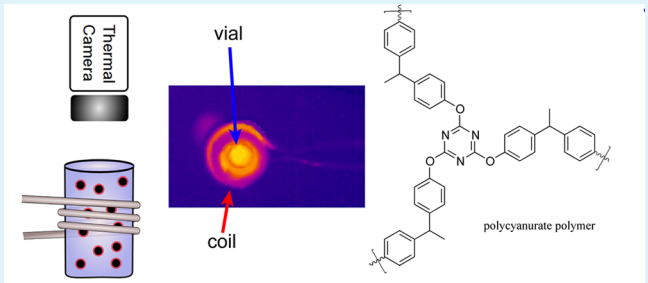

Heat Dissipation by Magnetic Nanoparticles in Alternating Magnetic Fields Promotes the Polymerization and Curing of a Cyanate Ester Resin

KEYWORDS: *polymerization, induction heating, magnetic nanoparticles, cyanate ester*

INTRODUCTION

The art of transforming a monomer into a synthetic polymer has been known for at least 100 years.[1] While the majority of polymerizations developed since that time use thermal heating, other alternatives are available including plasma-induced polymerization,[2] radiation-induced polymerization,[3] microwave induction heating,[4] dielectric heating,[5] and photoinduced thermal front polymerization.[6] Only recently have nanoparticles been embedded in a polymer matrix or coated with polymer for such purposes as drug delivery,[7] antimicrobial applications,[8] selective ultraviolet protection,[9] increasing polymer performance,[10] possible flame retardancy,[11] and many others.[12,13]

Mixtures of magnetic nanoparticles and polymers are now being used in combination with induction heating for a variety of purposes. Some examples include using nickel nanoparticles for bonding of composites[14] or induction curing[15] as well as polymerizations using iron oxide nanochains[16] or titanium nanoparticles.[17] Others have used larger particles in a magnetic field such as various sizes of nickel to study the heat generated by the particles in a polymer,[18] 1 μm of nickel alloy (Nitinol) used to compare polymerizations with conventional or induction heating,[19] or a variety of metal particles from 60 nm to 100 μm used for crack healing, remolding, or bonding of thermoreversible polymers.[20] Actuation of a reversible gel-to-

Received: August 22, 2013
Accepted: October 10, 2013
Published: October 10, 2013

sol transition using heating from chromium dioxide particles in a nanoparticle−polymer mixture in a magnetic field has been reported.[21] Interestingly, polymerization in a magnetic field without any particles has also been studied.[22]

Primaset LECy, or 1,1-bis(cyanatophenyl)ethane, is a cyanate ester resin that can be cured at elevated temperatures with a catalyst to form many useful products. As a group, cyanate esters tend to give materials with high glass transition temperatures (T_g)[23] and very low dielectric constants[24] as well as other useful properties such as low moisture absorption,[25] low volatility,[23] reduced toxicity,[26] resistance to fire,[27] and many others.[28] These properties make cyanate ester resins useful for a wide variety of fields such as applications in aerospace,[29,30] pressure-sensitive adhesives,[31] magnet insulation,[32] and electric insulators[33] as well as flexible circuitry, surface finishes, photonics, and biomedical applications.[28] Kessler et al. have studied the properties of bisphenol E cyanate ester nanocomposites with embedded nanoparticles of alumina,[34−36] silica,[37,38] zirconium tungstate,[39,40] and recently microparticles of iron oxide coated with silica[41] using standard polymerization techniques. An earlier study reported on the effects of layered silicates in LECy-based nanocomposites.[42] Similarly, the Gu group has investigated the properties of another cyanate ester resin mixed with carbon nanotubes,[43] aluminum nitride−carbon nanotubes,[44] zirconia fibers,[45] silica,[46] and organic rectorite, a layered silicate material.[47] There also exist reports on the properties of cyanate esters with layered silicate[48] or organoclay.[49] To our knowledge, there are no previous reports of polymerization of the LECy cyanate ester with nanoparticles used as the heat source.

Induction heating, heating of electrically conductive materials by electromagnet induction, historically was used for metal work[50] but recently has found many uses with magnetic nanoparticles.[15,51−53] Induction heating offers many advantages over traditional thermal heating such as the ability to heat only localized areas, the ability to reach high temperatures quickly, its high thermal efficiency, the ability to heat materials internally, and the fact that no contact is required with the material being heated.[18,54] One example where induction heating would have significant advantages, because of the ability to more readily control the temperature and uniformity of the heating, would be in the development of ultrahigh-molecular-weight polyethylene where formation temperatures are low to avoid melting and have been shown to affect the properties of the polymer.[55−57] The use of ferromagnetic and superparamagnetic particles as a localized heat source through the application of an alternating magnetic field can be found in a variety of examples,[14−20] but no instances are found using nanoparticles to drive the curing reaction of high-temperature thermosetting polymers. Here, we report the first polymerization of a high-temperature network polymer driven by the inductive heating of iron oxide nanoparticles dispersed within an uncured resin.

In general, polymerizations of cyanate esters are accomplished through thermal curing of the monomer with an initiator[58] or through photochemically initiated curing.[59] The thermal heating of the monomer is usually done with a slow heating ramp (2−5 K/min) to relatively high temperatures (150−300 °C) over a period of a few hours. The photochemical initiation can be done at room temperature, but the sample must be very thin and in most cases the reaction is highly oxygen-sensitive. Our use of magnetic nanoparticles in an alternating-current (ac) magnetic field as a heat source for polymerization avoids some of these difficulties.

EXPERIMENTAL SECTION

Iron(III) chloride hexahydrate (ACS reagent, 97%), iron(II) chloride tetrahydrate (ReagentPlus, 98%), tetramethylammonium hydroxide solution (25 wt % in water), and oleic acid (technical grade, 90%) were purchased from Sigma-Aldrich and used without further purification. Likewise, ammonium hydroxide (Certified ACS Plus, 28−30% by weight) and ethanol (anhydrous, histological) were purchased from Fisher Scientific and used without further purification. Primaset LECy [1,1-bis(4-cyanatophenyl)ethane] and a premade mixture of copper(II) acetylacetonate/nonylphenol (1:30 ratio) were provided by the Air Force Research Laboratory, Edwards Air Force Base, and used without further purification.

Preparation of Iron Oxide Magnetic Nanoparticles.[51] Iron(III) chloride hexahydrate (11.75 g, 43.5 mmol) and iron(II) chloride tetrahydrate (4.3 g, 21.6 mmol) were each separately dissolved in 100 mL of deionized, degassed water (bubbling nitrogen, 30 min), sonicated (30 min), and degassed with bubbling nitrogen (5 min). The two solutions were mixed in a 500 mL cylindrical reaction vessel with flat flange using a mechanical stirrer (100 rpm), and nitrogen was bubbled through the combined solution as it was heated to 70 °C. Once the solution reached 70 °C, ammonium hydroxide (30 mL) was added and the temperature was increased to 80 °C. The solution was held at 80 °C for 1 h, and deionized, degassed water and ammonium hydroxide were added as needed to compensate for evaporation and to maintain the reaction solution at pH 8. After 1 h, the heat was removed and the solution was allowed to reach room temperature. Aliquots (20 mL) were placed in 50 mL centrifuge tubes, centrifuged (1500 rpm, 312*g*) for 10 min, and magnetically decanted for the black particles.

To peptize the particles, tetramethylammonium hydroxide (10 mL) was added to each centrifuge tube, and the particles were suspended using a vortex, precipitated by centrifugation (10 min, 1500 rpm), and magnetically decanted. An additional portion of tetramethylammonium hydroxide (10 mL) was added to each tube, and the particles were suspended, precipitated, and collected. The black, tacky particles were transferred to a beaker, placed into an oven (60 °C), and dried overnight.

Coating of Iron Oxide Magnetic Nanoparticles.[55] A solution of the dried iron oxide peptized nanoparticles (7 g) and deionized water (280 mL), in a glass beaker, was placed in a sonicating water bath (20 min, Fisher Scientific Mechanical Ultrasonic Cleaner FS60) to suspend the particles and then into a high-intensity ultrasonic processor (5 min, Sonics Vibra-Cell VCX 750) to break any formed aggregates. Oleic acid (28 mL, 99.1 mmol) was added to the solution, which was again placed in the sonicating water bath (10 min). The solution was transferred to a 500 mL cylindrical reaction vessel with flat flange and heated (80 °C) with mechanical stirring (100 rpm). After 1 h, the heat was removed and the solution was allowed to reach room temperature. Aliquots (10 mL) of the colloid solution were placed in 50 mL centrifuge tubes, and ethanol (35 mL) was added to each tube. The tubes were centrifuged (7500 rpm, 7800*g*) for 15 min and magnetically decanted for the black particles. The oleic acid coated iron oxide nanoparticles were removed from the centrifuge tubes and dried in air. The dried nanoparticles were stored in a refrigerator at 4 °C.

Polymerization of Primaset LECy Using Induction Heating. Oleic acid coated iron oxide nanoparticles (10.5 mg), a premixed (1:30 ratio) copper(II) acetylacetonate/nonylphenol catalytic system (41.4 mg), and LECy (1.00 g) were added to a 4 mL glass vial and mixed using a vortex (30 s). The materials were further mixed using a sonicating water bath (20 min, Branson Ultrasonic Cleaner B200), then degassed by sonication (30 min, Cole-Parmer Ultrasonic Cleaner 889O-DTH, degas setting), and further suspended by the sonicating water bath (5 min). The vial was quickly placed in the induction heater and the temperature measured from above using a thermal camera (FLIR Systems ThermoVision A20). The reaction vial was held in the

induction heater coil, as well as insulated, by a handmade Styrofoam piece shaped to fit the coil. The induction heater was controlled using the power setting that corresponds to the following: adjusting the voltage and ramping to 90 °C, holding at that temperature for 1 h, then ramping to 120 °C or the highest temperature achieved with maximum power, and holding for an additional 1 h. After cooling, the vial was removed from the induction heater and the formed polymer was characterized.

Polymerization of Samples in a Laboratory Oven. Premixed (1:30 ratio) copper(II) acetylacetonate/nonylphenol (0.04 g) and LECy (1.00 g) were added to a vial and mixed by hand for a few minutes to achieve uniformity. The liquid mixture was then degassed at 300 mmHg for 30 min at room temperature. The degassed mixture was then poured into a silicone mold (RZ2364A/B from Silpak, Inc.) cured overnight at room temperature followed by 1 h at 160 °C and finally placed in a Carbolite convection oven with the temperature monitored by an internal thermocouple. To mimic the actual temperature profile from the induction heating experiments, the oven was ramped at 5 °C/min to 90 °C and then held at 90 °C for 1 h. Following this, the oven was ramped at 5 °C/min to 110 °C and held at 110 °C for 1 min. The setpoint was then reduced to 105 °C and held for 1 h. During this period, the temperature slowly drifted downward, reaching 105 °C in a few minutes. This profile mimics the sample temperature seen in Figure 3.

RESULTS AND DISCUSSION

The general synthetic strategy, as illustrated in Figure 1, is mixing magnetic nanoparticles, the LECy monomer, and an initiator consisting of a mixture of copper(II) acetylacetonate [$Cu(acac)_2$] and nonylphenol and then placing the mixture in an alternating magnetic field of selected frequency and amplitude for a given time. The temperature is monitored by a thermal camera placed directly above the sample. This procedure has the advantages of allowing temperatures to be reached quickly, the sample being heated uniformly inside the coil and from within instead of by external heating, allowing for lower temperatures to be used, and the process just lasting 2 h. Recent, not yet characterized, reactions suggest that a much quicker polymerization time is also possible. Detailed reaction conditions can be found in the Experimental Section, but the procedure is summarized here. In a 4 mL glass sample vial was weighed, in order, iron oxide nanoparticles (1% w/w), then 4 phr of premixed $Cu(acac)_2$/nonylphenol (1:30 ratio) initiator, and finally LECy monomer. $Cu(acac)_2$/nonylphenol is a widely used catalyst system for cyanate esters[60] in which the nonylphenol provides a proton source to initiate cyclotrimerization and the copper compound acts as an accelerator. The mixture was sonicated for 20 min, degassed by sonication for 30 min, and sonicated again for an additional 5 min. The vial was quickly placed in the induction heater coil, and an appropriate field was applied to hold the temperature at 90 °C for about 1 h and then 120 °C for another 1 h, at which time the vial was cooled to room temperature and the polymer characterized. The field amplitude needed at the various stages of polymerization depended on the concentration of the particles in the mixture and their intrinsic heating rate.

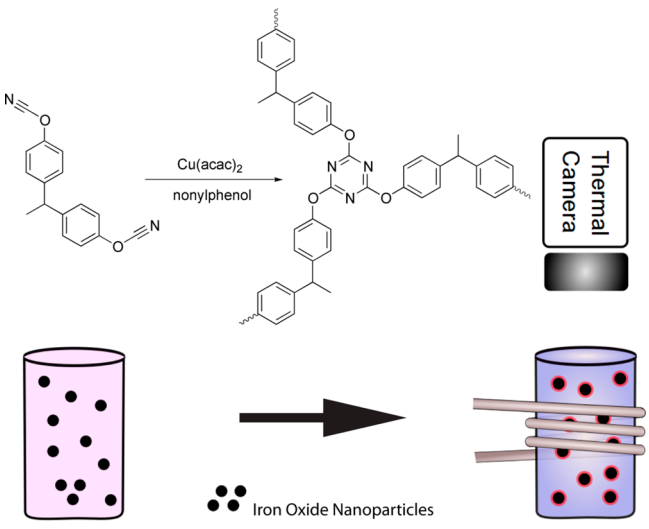

Figure 1. Polymerization reaction scheme showing the structure of the Primaset LECy monomer and formed polymer as well as a graphical representation of the mixture being heated in the coil used for induction heating.

The magnetic nanoparticles used for this polymerization were synthesized by the coprecipitation method[61] because of the relative ease of producing and functionalizing the surface of the particles. While some aggregation is expected from the coprecipitation and coating procedures, the advantages are that it is much simpler than the thermodecomposition heating-up method and more economical and the particles generally produce more heat in an induction heater compared to similarly sized particles from the thermodecomposition method. Iron(II) and iron(III) salts were coprecipitated in ammonium hydroxide under nitrogen and then peptized using tetramethylammonium hydroxide. After drying, the particles were coated with oleic acid using an adsorption reaction in water with sonication to form colloidally stable particles. Other ligands were tested, such as (3-aminopropyl)triethoxysilane and 3-(trimethoxysilyl)propyl methacrylate, but the magnetic nanoparticles coated with oleic acid were the particles that suspended the most readily and stayed suspended the longest in the LECy monomer. The coated particles were characterized by powder X-ray diffraction (XRD), superconducting quantum interference device (SQUID) magnetometry, thermogravimetric analysis, and dynamic light scattering (DLS). The particle size was measured and gave a magnetic core of 9 nm (SQUID), a core of 13.7 nm (transmission electron microscopy, TEM), and a hydrodynamic diameter of 32 nm (DLS). Detailed synthetic steps and relevant data for the magnetic nanoparticles can be found in the text and the Supporting Information (SI).

To characterize the energy dissipation rate properties of the magnetic nanoparticles, the specific absorption rate (SAR)[62] was determined by suspending the particles in the LECy monomer and placing them in magnetic fields of different amplitudes. In general, the SAR can be understood to mean the heating capacity of a particular material due to induction heating and is measured in watts per gram of material (W/g). Figure 2 shows the observed temperature increase with respect to time for six magnetic field amplitudes for 10.1 mg of magnetic nanoparticles in 1.01 mL of LECy. The general trend is an increase in the rate of heating with increasing magnetic field strength. SAR values and calculations are available in the SI.

The alternating magnetic field used for polymerization of the LECy monomers was generated using a HFI 3 kW RF heating system manufactured by RDO Induction Power Supplies, and the temperature at the surface of the polymerization was measured using a FLIR ThermoVision A20 infrared thermal camera. The coil used to create the magnetic field was a 4-turn solenoid coil made from 3.2 mm ($^1/_8$ in.) copper tubing with an outer diameter of 34 mm and a height of 30 mm. The surface

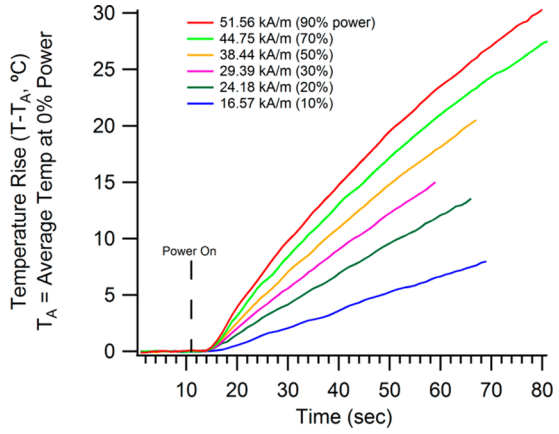

Figure 2. Initial rates of temperature rise as a function of the field amplitude at selected induction heater power plotted as a change in the temperature versus time. All experiments were run at a frequency of 233 kHz. The initial rate increases are used in the SAR calculations (see the SI).

temperatures of the sample, coil, and environment were captured and then plotted as a function of time, as shown in Figure 3. The target was to heat the material to 90 °C for 1 h and then increase the temperature to 120 °C for an additional 1 h. As seen in Figure 3d, the surface temperature of the polymerization sample was held at 90 °C by adjusting the power of the induction heater as needed and then was raised to the maximum power possible in the induction heater. For the experiment shown in Figure 3d, the highest temperature reached was about 110 °C, but other experiments were held at or above 120 °C. As would be expected, experiments showed that a higher weight percent of magnetic nanoparticles (2% or 3%) requires much less power to reach the desired temperature and can also reach the temperature sooner. A similarly prepared sample without nanoparticles was tested in the induction heater; no significant rise in the temperature was observed, and the sample did not polymerize after 2 h. Those results and the large difference in the sample and coil temperatures seen in Figure 3d, signifying that energy would flow from the sample to the coil and not vice versa, indicate that the resin is cured through heat generated by the magnetic nanoparticles.

Magnetic nanoparticles respond to alternating magnetic fields to dissipate heat through two mechanisms: Brownian motion and Néel relaxation. The Brownian contribution is due to rotation of the particles in a fluid and depends on the viscosity of the fluid and hydrodynamic volume of the particle. In contrast, the Néel contribution is due to internal dipole rotation and depends on the magnetocrystalline anisotropy, which depends on the nature of the magnetic material, and the magnetic volume of the particle. It is likely that both Brownian motion and Néel relaxation contribute to the initial heating of the particles, but as the viscosity of the monomer increases, the Brownian contribution would decrease. This is suggested by the need to increase the power of the induction heater to maintain a constant temperature as well as the slight decrease in the surface temperature during the second hour of heating at maximum induction heater power.

The polymer that formed after induction heating was a glassy solid at room temperature and had an opaque glossy black color due to the embedded nanoparticles. While the bulk polymer was opaque and not much detail could be seen, when the sample was sectioned for characterization by TEM, the polymer appeared transparent orange and small parallel aggregates could be seen with the naked eye, mainly near the outer edge of the polymer (see the SI). For comparison, a polymer sample produced from the thermal curing of LECy that did not contain nanoparticles was a transparent, light-orange color. Once thinly sliced, the polymer produced through induction heating looked no different to the naked eye than the polymer made through convection heating with the obvious addition of nanoparticles.

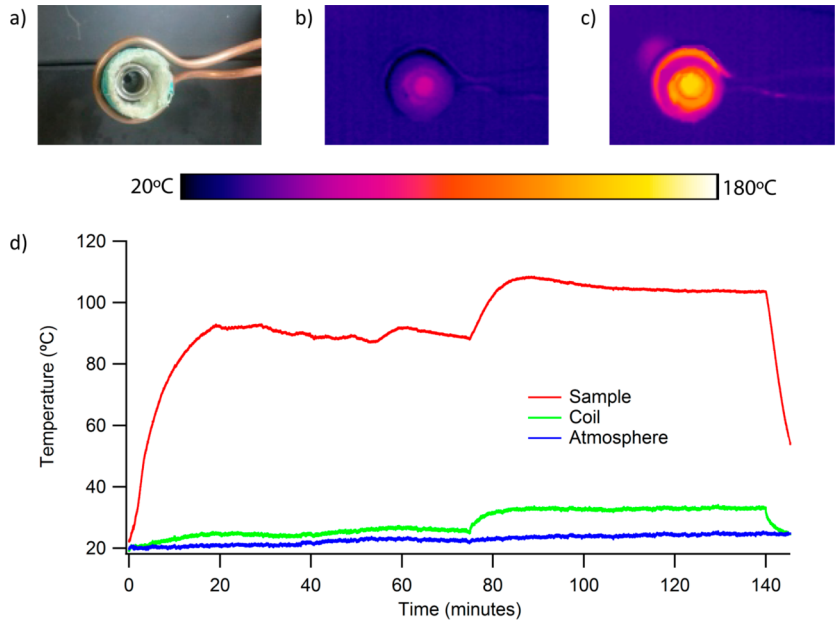

Figure 3. View from above the sample in the coil for induction heating shown (a) as a picture before heating, (b) as a thermal image before the ac magnetic field is applied, and (c) as a thermal image after the AC magnetic field is applied. (d) Plot of the temperatures of the sample, induction heating coil, and atmosphere versus time.

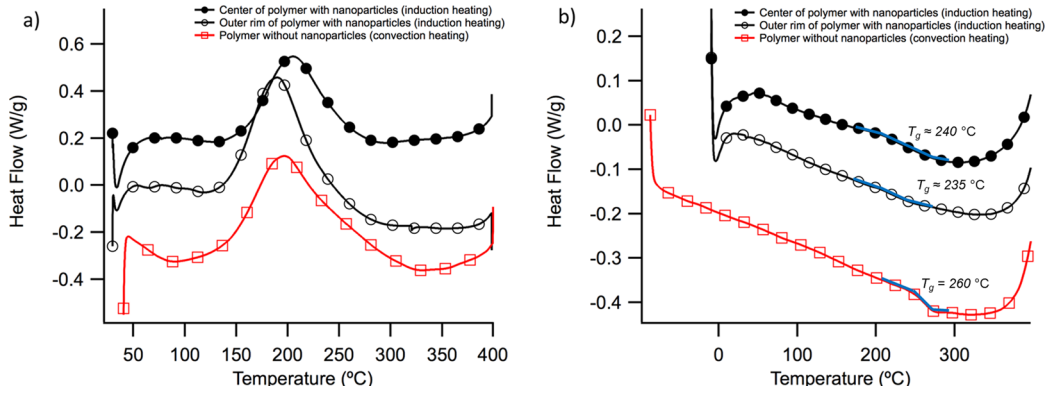

Figure 4. DSC thermograms of LECy samples cured by induction heating with dispersed magnetic nanoparticles (black lines) and cured by traditional convection heating (red line). The initial temperature scans of the "as-cured" material (a) show exothermic curves in all three samples representing unreacted monomer with a peak exotherm around 200 °C. The second temperature scans of the fully cured (by the initial scan to 400 °C) material (b) show a T_g of around 260 °C for the three curves.

Differential scanning calorimetry (DSC) was used to understand the degree of cure attained by induction heating of the dispersed magnetic nanoparticles. Figure 4 shows DSC thermograms of inductively cured LECy with dispersed magnetic nanoparticles as well as a LECy sample cured traditionally in a normal laboratory oven with the same temperature history. Two samples were taken from the inductively cured LECy, the first from the outer edge containing some aggregates of the magnetic nanoparticles and the second from the center where the magnetic nanoparticles were well dispersed, as seen by TEM (Figure 5). During the initial temperature scan, each of these samples showed an exothermic peak around 200 °C and a similar conversion percentage (Figure 4a). The DSC showed that the samples formed through induction heating had a slightly higher conversion, but the difference between them and the sample formed with convection heating was within the measurement uncertainty. Temperature scans of the inductively cured material taken from the center (homogenous particle dispersion) and edge of the sample (some particle agglomeration) showed integrated residual heats of reaction of around 90 and 70 kJ/mol, respectively. Previous experience has shown that this type of DSC analysis of cyanate ester systems gives an uncertainty of about 10 kJ/mol. A cure scan of the LECy monomer containing an identical amount of catalyst and nanoparticles shows an integrated heat of reaction of around 230 kJ/mol, indicating that the induction curing method drove the curing reaction to conversions of 65−70% (±5%).

A 65% conversion using induction heating through the use of iron oxide magnetic nanoparticles would likely necessitate a postcure in industrial applications. However, the conversion is large enough for samples to be demolded without distortion at room temperature and brought to higher conversion as free-standing parts. On the basis of a previous study,[29] a conversion of 65% is consistent with the times and temperatures utilized. They report that curing LECy with 2 phr of the same catalyst mixture in a laboratory oven for 1 h at 125 °C gives a conversion of 57%, curing for 2 h at 125 °C shows a conversion of 73%, and longer cure times (12 h) give a 76% conversion rate. This shows our conversion rate to be in good agreement with other cure data for LECy and suggests that a conversion of 85% or greater, usually desired for optimal performance, could be achieved by further optimization of the process.

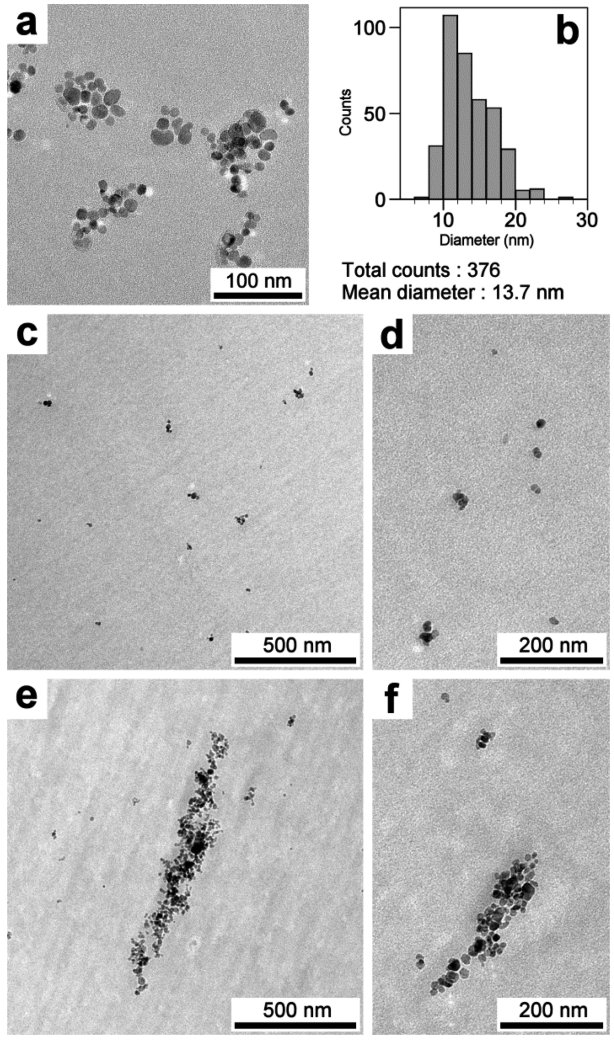

Figure 5. TEM micrographs of the nanoparticles used in these polymerizations (a) with the corresponding size distribution graph (b). Ultrathin sections of the polymer: (c) dispersed nanoparticles, sometimes forming small aggregates; (d) higher-magnification image showing dispersed nanoparticles; (e) elongated aggregates of nanoparticles; (f) higher-magnification image showing elongated aggregates.

dx.doi.org/10.1021/am4035575 | ACS Appl. Mater. Interfaces 2013, 5, 11329−11335

Figure 4b shows the second temperature scan in DSC for the three samples and that the glass transition temperature T_g of fully cured material (by the initial heating scan to 400 °C) is not strongly affected by the presence of the magnetic nanoparticles. All of the samples have a T_g of around 260 °C, which is within the expected range for fully cured LECy with a 4 phr catalyst mixture. After heating to 400 °C, the T_g values for the inductively cured samples are slightly lower than those for the oven-cured sample and are less distinct. These differences may be caused by a small amount of retained water that is released upon heating to temperatures above 200 °C. At these elevated temperatures, water will react with uncured cyanate ester groups to produce carbamates while also hydrolyzing a small portion of the cyanurate linkages. Both reactions involving water will degrade the network structure, resulting in a lower and less distinct glass transition temperature. However, this modest difference in T_g is only seen when the samples are heated to well above their cure temperature, whereas there are not significant differences between the three samples in the "as-cured" state. This DSC data demonstrate that the samples produced using induction heating have the same physical properties, such as conversion amount, and the same useful cure and solidification effects as those produced using oven heating while providing all of the previously stated advantages of an induction cure.

The material was also characterized by TEM, after ultrathin sectioning, to determine the dispersion of the nanoparticles in the polymer (Figure 5). The particles were mainly dispersed (Figure 5c,d), but small aggregates of a few particles were observed throughout and larger elongated aggregates were observed mainly near the outer edge of the polymer, corresponding to those seen with the naked eye (Figure 5e,f). It is not clear whether these aggregates would increase[63] or decrease[64] the magnetic susceptibility and heat output of the particles.

CONCLUSIONS

In this article, we have presented the synthesis of a polycyanurate polymer from the commercial monomer Primaset LECy using magnetic iron oxide nanoparticles in an ac field as an internal heat source. The formed polymer showed both the same conversion and T_g expected, based on the thermal history, as those of the polymer formed from convection heating without nanoparticles. These results are a good indication that the nanoparticles are not interfering with the expected cure chemistry and that fabrication of a high-T_g, high-thermal-stability thermoset using induction heating is possible. The TEM images showed the magnetic nanoparticles mostly well dispersed with some aggregation. Additional characterizations, including the nanocomposite mechanical strength compared to the thermally synthesized polymer, as well as optimization of the reaction conditions are needed. However, the experiments reported here indicate that this approach could be a promising alternative for thermal curing of cyanate ester resins such as Primaset LECy.

ASSOCIATED CONTENT

Supporting Information

Characterization details of the magnetic nanoparticles including instrumentation used and results obtained as well as all calculated SAR values and additional TEM images. This material is available free of charge via the Internet at http://pubs.acs.org.

AUTHOR INFORMATION

Corresponding Author

*E-mail: carlos.rinaldi@bme.ufl.edu.

Notes

The authors declare no competing financial interest.

ACKNOWLEDGMENTS

The authors thank Ana C. Bohorquez for providing the oleic acid coated iron oxide nanoparticles used in this paper and Lorena Maldonado-Camargo for XRD characterization. Funding and materials from the Air Force Research Laboratory, Edwards Air Force Base, CA, are also gratefully acknowledged. We also appreciate support of the University of Puerto Rico (UPR), NSF, and NASA for the Nanoscopy Facility, a user facility at UPR.

REFERENCES

(1) Baekeland, L. H. Method of Making Insoluble Products of Phenol and Formaldehyde. U.S. Patent 942,699, 1909.
(2) Kim, S. Y.; Kanamori, T.; Shinbo, T. *J. Appl. Polym. Sci.* **2002**, *84*, 1168−1177.
(3) Çaykara, T.; Özyürek, C.; Kantoğlu, Ö. *J. Appl. Polym. Sci.* **2007**, *103*, 1602−1607.
(4) Mallakpour, S.; Zadehnazari, A. *J. Macromol. Sci., Part A: Pure Appl. Chem.* **2009**, *46*, 783−789.
(5) Ioanid, G. E.; Neamtu, I. *J. Optoelectron. Adv. Mater.* **2007**, *9*, 965−969.
(6) Nason, C.; Pojman, J. A.; Hoyle, C. *J. Polym. Sci., Part A: Polym. Chem.* **2008**, *46*, 8091−8096.
(7) Patel, T.; Zhou, J.; Piepmeier, J. M.; Saltzman, W. M. *Adv. Drug Delivery Rev.* **2012**, *64*, 701−705.
(8) Perreault, F.; Oukarroum, A.; Melegari, S. P.; Matias, W. G.; Popovic, R. *Chemosphere* **2012**, *87*, 1388−1394.
(9) Calvo, M. E.; Castro Smirnov, J. R.; Míguez, H. *J. Polym. Sci., Part B: Polym. Phys.* **2012**, *50*, 945−956.
(10) Vaia, R. A.; Maguire, J. F. *Chem. Mater.* **2007**, *19*, 2736−2751.
(11) Kashiwagi, T.; Morgan, A. B.; Antonucci, J. M.; Van Landingham, M. R.; Harris, R. H.; Awad, W. H.; Shields, J. R. *J. Appl. Polym. Sci.* **2003**, *89*, 2072−2078.
(12) Sanchez, C.; Belleville, P.; Popall, M.; Nicole, L. *Chem. Soc. Rev.* **2011**, *40*, 696−753.
(13) Ghosh Chaudhuri, R.; Paria, S. *Chem. Rev.* **2012**, *112*, 2373−2433.
(14) Suwanwatana, W.; Yarlagadda, S.; Gillespie, J. W., Jr. *Compos. Sci. Technol.* **2006**, *66*, 1713−1723.
(15) Ye, S.; Cramer, N. B.; Stevens, B. E.; Sani, R. L.; Bowman, C. N. *Macromolecules* **2011**, *44*, 4988−4996.
(16) Ma, M.; Zhang, Q.; Dou, J.; Zhang, H.; Yin, D.; Geng, W.; Zhou, Y. *J. Colloid Interface Sci.* **2012**, *374*, 339−344.
(17) Barthélémy, B.; Devillers, S.; Minet, I.; Delhalle, J.; Mekhalif, Z. *J. Colloid Interface Sci.* **2011**, *354*, 873−879.
(18) Suwanwatana, W.; Yarlagadda, S.; Gillespie, J. W., Jr. *Compos. Sci. Technol.* **2006**, *66*, 2825−2836.
(19) Devillers, S.; Barthélémy, B.; Delhalle, J.; Mekhalif, Z. *ACS Appl. Mater. Interfaces* **2011**, *3*, 4059−4066.
(20) Bowman, C.; Adzima, B.; Kloxin, C. Radio Frequency Magnetic Responsive Polymer Composites. U.S. Patent Application 13/303,782, June 28, 2012.
(21) Adzima, B. J.; Kloxin, C. J.; Bowman, C. N. *Adv. Mater.* **2010**, *22*, 2784−2787.
(22) Nita, L. E.; Chiriac, A. P.; Cimmino, S.; Silvestre, C.; Duraccio, D.; Vasile, C. *Open Macromol. J.* **2008**, *2*, 26−31.
(23) Guenthner, A. J.; Davis, M. C.; Lamison, K. R.; Yandek, G. R.; Cambrea, L. R.; Groshens, T. J.; Baldwin, L. C.; Mabry, J. M. *Polymer* **2011**, *52*, 3933−3942.
(24) Goertzen, W. K.; Kessler, M. R. *Composites, Part A* **2007**, *38*, 779−784.

(25) Hillermeier, R. W.; Seferis, J. C. *J. Appl. Polym. Sci.* **2000**, *77*, 556−567.
(26) Guenthner, A. J.; Lamison, K. R.; Vij, V.; Reams, J. T.; Yandek, G. R.; Mabry, J. M. *Macromolecules* **2012**, *45*, 211−220.
(27) Cambrea, L. R.; Davis, M. C.; Groshens, T. J.; Guenthner, A. J.; Lamison, K. R.; Mabry, J. M. *J. Polym. Sci., Part A: Polym. Chem.* **2010**, *48*, 4547−4554.
(28) Fang, T.; Shimp, D. A. *Prog. Polym. Sci.* **1995**, *20*, 61−118.
(29) Reams, J. T.; Guenthner, A. J.; Lamison, K. R.; Vij, V.; Lubin, L. M.; Mabry, J. M. *ACS Appl. Mater. Interfaces* **2012**, *4*, 527−535.
(30) Voicu, R. *Mater. Plast.* **2012**, *49*, 34−40.
(31) Hreha, R. D.; Collins, B. N. Cyanate ester-based pressure sensitive adhesive. Eur. Patent Application 10169538.5, Oct 12, 2011.
(32) Hooker, M. W.; Arzberger, S. A.; Grandlienard, S. D.; Stewart, M. W.; Munshi, N. A.; Voss, G. M.; Benson, R. D.; Madhukar, M. S. *IEEE Trans. Appl. Supercond.* **2009**, *19*, 2367−2370.
(33) Pietrowicz, S.; Four, A.; Canfer, S.; Jones, S.; Baudouy, B. *AIP Conf. Proc.* **2012**, *1434*, 1976−1982.
(34) Sheng, X.; Akinc, M.; Kessler, M. R. *Mater. Sci. Eng., A* **2010**, *527*, 5892−5899.
(35) Sheng, X.; Akinc, M.; Kessler, M. R. *Polym. Eng. Sci.* **2010**, *50*, 302−311.
(36) Ament, K. A.; Kessler, M. R.; Akinc, M. *Polym. Eng. Sci.* **2011**, *51*, 1409−1417.
(37) Sheng, X.; Akinc, M.; Kessler, M. R. *Polym. Eng. Sci.* **2010**, *50*, 1075−1084.
(38) Sun, W.; Eliseo De León, J.; Ma, C.; Tan, X.; Kessler, M. R. *Compos. Sci. Technol.* **2012**, *72*, 1692−1696.
(39) Badrinarayanan, P.; Kessler, M. R. *Compos. Sci. Technol.* **2011**, *71*, 1385−1391.
(40) Badrinarayanan, P.; Rogalski, M. K.; Kessler, M. R. *ACS Appl. Mater. Interfaces* **2011**, *4*, 510−517.
(41) Sun, W.; Sun, W.; Kessler, M. R.; Bowler, N.; Dennis, K. W.; McCallum, R. W.; Li, Q.; Tan, X. *ACS Appl. Mater. Interfaces* **2013**, *5*, 1636−1642.
(42) Wooster, T. J.; Abrol, S.; MacFarlane, D. R. *Polymer* **2005**, *46*, 8011−8017.
(43) Wang, B.; Liang, G.; Jiao, Y.; Gu, A.; Liu, L.; Yuan, L.; Zhang, W. *Carbon* **2013**, *54*, 224−233.
(44) Mi, Y.-n.; Liang, G.; Gu, A.; Zhao, F.; Yuan, L. *Ind. Eng. Chem. Res.* **2013**, *52*, 3342−3353.
(45) Qin, D.; Gu, A.; Liang, G.; Yuan, L. *RSC Adv.* **2012**, *2*, 1364−1372.
(46) Hu, J.-t.; Gu, A.; Liang, G.; Zhuo, D.; Yuan, L. *Polym. Adv. Technol.* **2012**, *23*, 454−462.
(47) Yuan, L.; Gu, A.; Liang, G.; Ma, X.; Lin, C.; Chen, F. *Polym. Eng. Sci.* **2012**, *52*, 2443−2453.
(48) Ganguli, S.; Dean, D.; Jordan, K.; Price, G.; Vaia, R. *Polymer* **2003**, *44*, 1315−1319.
(49) Mondragón, I.; Solar, L.; Nohales, A.; Vallo, C. I.; Gómez, C. M. *Polymer* **2006**, *47*, 3401−3409.
(50) Lozinskii, M. G. e. *Industrial Applications of Induction Heating*; Pergamon Press: New York, 1969; p 672.
(51) Creixell, M.; Bohórquez, A. C.; Torres-Lugo, M.; Rinaldi, C. *ACS Nano* **2011**, *5*, 7124−7129.
(52) Terrisa, D.; Andrew, E.; Karen, C.; Matt, C.; Vishnu Baba, S.; Fred, W.; Erin, B. M.; Ajit, M.; James, R. A.; Aaron, C.; Teng, K. O. Smart Self-Healing Material Systems Using Inductive and Resistive Heating. *Smart Coatings III*; American Chemical Society: Washington, DC, 2010; Vol. *1050*, pp 45−60.
(53) Sonoda, A.; Nitta, N.; Nitta-Seko, A.; Ohta, S.; Takamatsu, S.; Ikehata, Y.; Nagano, I.; Jo, J.-i.; Tabata, Y.; Takahashi, M.; Matsui, O.; Murata, K. *Int. J. Nanomed.* **2010**, *5*, 499−504.
(54) Zinn, S. S.; Lee, S. *Elements of Induction Heating: Design, Control, and Applications*; ASM International: Palo Alto, CA, 1988; p 335.
(55) Yeh, J.-T.; Lin, Y.-T.; Chen, K.-N. *J. Appl. Polym. Sci.* **2003**, *89*, 3728−3738.
(56) Jian, T.; Shyu, W.-D.; Lin, Y.-T.; Chen, K.-N.; Yeh, J.-T. *Polym. Eng. Sci.* **2003**, *43*, 1765−1777.
(57) Yeh, J.-T.; Wang, C.-K.; Yeh, A.; Huang, L.-K.; Wang, W.-H.; Hsieh, K.-H.; Huang, C.-Y.; Chen, K.-N. *Polym. Int.* **2013**, *62*, 591−600.
(58) Crawford, A. O.; Howlin, B. J.; Cavalli, G.; Hamerton, I. *React. Funct. Polym.* **2012**, *72*, 596−605.
(59) Kotch, T. G.; Lees, A. J.; Fuerniss, S. J.; Papathomas, K. I. *Chem. Mater.* **1995**, *7*, 801−805.
(60) Hamerton, I., Ed. *Chemistry and Technology of Cyanate Ester Resins*; Blackie Academic: New York, 1994; p 357.
(61) Massart, R. *IEEE Trans. Magn.* **1981**, *17*, 1247−1248.
(62) Jordan, A.; Rheinländer, T.; Waldöfner, N.; Scholz, R. *J. Nanopart. Res.* **2003**, *5*, 597−600.
(63) Dennis, C. L.; Jackson, A. J.; Borchers, J. A.; Ivkov, R.; Foreman, A. R.; Lau, J. W.; Goernitz, E.; Gruettner, C. *J. Appl. Phys.* **2008**, *103*, 07A319-3.
(64) Serantes, D.; Baldomir, D.; Martinez-Boubeta, C.; Simeonidis, K.; Angelakeris, M.; Natividad, E.; Castro, M.; Mediano, A.; Chen, D. X.; Sanchez, A.; Balcells, L. I.; Martinez, B. *J. Appl. Phys.* **2010**, *108*, 073918−5.